Available online at www.sciencedirect.com
ScienceDirect
Scripta Materialia 64 (2011) 319–322
Scripta MATERIALIA
www.elsevier.com/locate/scriptamat

On tuning the morphology of nanoporous gold

E. Detsi, M. van de Schootbrugge, S. Punzhin, P.R. Onck and J.T.M. De Hosson*

Department of Applied Physics, Zernike Institute for Advanced Materials, University of Groningen, Nijenborgh 4, 9747 AG Groningen, The Netherlands

Received 24 July 2010; revised 23 September 2010; accepted 18 October 2010
Available online 5 November 2010

This paper concentrates on tuning the morphology of nanoporous metals, in particular Au, as a function of the dealloying potential. Ligament diameter and pore size were evaluated from digital image analysis and from measurements taken directly from scanning electron micrographs. Linear relationships were observed between the dealloying potential and the size of ligaments and pores. At a low dealloying potential the pore size is larger than the ligament diameter but at a high dealloying potential they are comparable.

Keywords: Nanoporous metal; Alloys; Au; Scanning electron micrographs

So far, the most popular method for controlling the morphology of nanoporous metals [1–9] is by coarsening of ligaments and pores during thermal or acid post-treatments, where nanoporous specimens are either exposed to high temperatures or kept in an acid environment after dealloying [10–14]. In the case of nanoporous gold, the coarsening of ligaments and pores is driven by the reduction of surface energy, which involves surface diffusion of gold atoms in order to form nanoporous structures with minimal surface energy [10]. Although ultrafine nanoporous gold structures can be achieved during dealloying at very low temperature (down to −20 °C) [15], thermal or acid coarsening is generally used as a post-dealloying treatment to increase the size of ligaments and pores. The objective of this study is to show that during dealloying the control potential can be tuned so as to synthesize ultrafine nanoporous gold structures as well as nanoporous gold with larger ligament and pore sizes. In our work, a linear relation is found between the dealloying potential and the size of ligaments and pores, in a potential range between 0.8 and 1.3 V, with respect to an Ag/AgCl reference electrode.

An electrical current can be used to follow the evolution of the dealloying process. When an Au–Ag alloy is used as the anode in an electrochemical cell, anodic oxidation occurs if a potential difference is maintained at the electrodes. Silver oxidation represents one of the principal reactions that takes place in the electrochemical cell during the dealloying process, but also other processes may occur; each silver atom from the anode loses one electron and forms a silver ion as described by $Ag(s) \rightarrow Ag^{+} + e^{-}$. The positive silver ion moves through the electrolyte to the cathode, where it is electrodeposited, provided the dealloying potential is higher than the reduction potential for silver formation. In contrast to silver ions, electrons do not move to the cathode through the electrolyte but via the external circuit containing the voltage supplier. An ammeter connected in series with the voltage supplier detects a current generated by these electrons. For an Au–Ag alloy, where only silver atoms dissolve in the electrolyte, the current probed by the ammeter represents the silver dissolution current. Figure 1a displays six different dissolution current intensities recorded during dealloying of six identical Au–Ag foils at different electrode potentials, using a three-electrode electrochemical cell. At the end of each process the dealloying current intensity drops down to a few microamperes. At 0.8 V, the dissolution process takes about 15 h but at 1.3 V it takes about 1 h, meaning that the rate of silver atom dissolution in the electrolyte is higher at high potentials.

The morphological changes of nanoporous gold as a function of the dealloying potential were investigated in a set of six nanoporous gold films dealloyed at different potentials. Gold foils from Noris Blattgold GmbH with a thickness of ~2 μm were used. The six specimens had the same composition ($Au_{25}Ag_{75}$ wt.%), the same rectangular geometry (15 × 5 mm^2) and the same initial weight (1.5 ± 0.2 mg). Selective dissolution of silver was performed in 1 M perchloric acid at room temperature,

* Corresponding author. Tel.: +31 503634897; fax: +31 503634 881; e-mail: j.t.m.de.hosson@rug.nl

1359-6462/$ - see front matter © 2010 Acta Materialia Inc. Published by Elsevier Ltd. All rights reserved.
doi:10.1016/j.scriptamat.2010.10.023

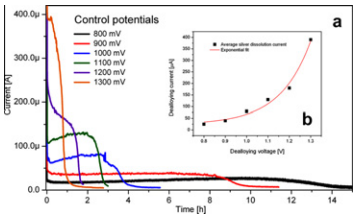

Figure 1. (a) Dealloying current intensity of each specimen as a function of the dealloying time. (b) Corresponding changes in the average silver dissolution current as a function of the dealloying voltage.

using a three-electrode electrochemical cell. Silver dissolution from each specimen was controlled by a potential chosen between 0.8 and 1.3 V generated by a potentiostat (microAutolab III/FRA2, Eco Chemie) and measured against an Ag/AgCl reference electrode (6.0733.100, Eco Chemie) kept at ~5 cm from the working electrode. Figure 1a shows the dealloying current intensities for each specimen as a function of the dealloying time. The corresponding changes in the average silver dissolution current (which is here referred to the constant dissolution current from a dealloying curve) and changes in nanoporous gold morphology as a function of the applied potentials are displayed in Figures 1b and 2, respectively. An exponential increase in silver dissolution current intensity with increasing control potential is observed (Fig. 1b). Morphological changes are observed on the set of six dealloyed specimens. Qualitatively, the scanning electron micrographs in Figure 2 show that the size of the ligaments and pores decreases with increasing control potential. That behavior is in agreement with the model on porosity evolution proposed by Erlebacher et al. [1,2], according to which the characteristic spacing between gold clusters, established at the beginning of the dealloying process, decreases with increasing overpotential. The ratio of the pore diameters to the ligament sizes as a function of the potential is constant within error bars. The homogeneity of the porous morphology as displayed in Figure 2 was investigated throughout the entire sample surface and also in cross-sections. The structure in the bulk of the sample was identical to the one at the sample surface. Due to this morphological homogeneity, the structure size of a sample could be investigated at any location.

Homogeneous areas of 300 × 290 pixels, corresponding to 629 × 608 nm^2, were captured from each scanning electron micrograph of Figure 2 for image analysis.

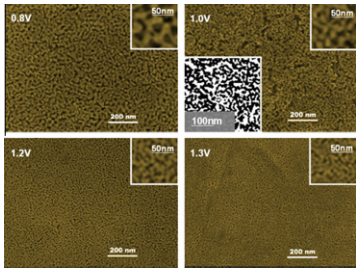

Figure 2. Scanning electron micrographs showing qualitative changes in nanoporous gold morphology as a function of the applied potentials. A snapshot of the digitized image for the specimen dealloyed at 1.0 V is shown.

Each area was selected so as to avoid cracks as much as possible. The corresponding images were converted into black (pore) and white (ligament) pixels for image analysis using Matlab. A snapshot of a typical digitized image is shown in Figure 2 for the specimen dealloyed at 1.0 V. Due to the random orientation of ligaments and pores in three-dimensional nanoporous gold, it is difficult to extract reliable quantitative information on the size of ligaments and pores from a two-dimensional (2-D) binarized image. However, a set of six binary images associated with the six specimens clearly indicates differences in morphology, meaning that, for a comparative study, useful information on the characteristic size of ligaments and pores could be extracted from 2-D binary images.

A difficulty encountered during image processing is the evaluation of the grayscale threshold value associated with the exact distance between black and white pixels [16]. However, possible overestimation of the ligament and pore sizes due to an inaccurate threshold grayscale value is not expected to affect the comparative study on the morphology of the six specimens, as long as the same grayscale threshold value and other image processing parameters, including brightness and contrast, are used throughout the analyses. Ligament and pore size counts were achieved by moving 290 times along the 300 pixel lines, forming a 300 × 290 captured pixels area, and recording the numbers of pixels falling in the white and black phases. Ligament and pore size counts for each specimen are plotted in Figure 3a and b, respectively. The corresponding changes in ligament and pore size vs. control potential is shown in Figure 3c, where the open circles represent the ligament size peaks (highest count) and the filled circles represent the pore size peaks (highest count).

As shown in Figure 3c, the size of the ligaments (peaks) decreases from ~22 to ~10 nm when the control potential is increased from 0.8 to 1.3 V. Similarly, the size of the pores (peaks) decreases from ~16 to ~9 nm under similar dealloying conditions. Note that, from the digitized images, ligaments appear to be larger than pores. That trend does not really hold for the two specimens dealloyed at 0.9 and 1 V. In particular, the specimen dealloyed at 1 V has pore sizes larger than the ligament sizes, as shown in Figure 3c. That exception

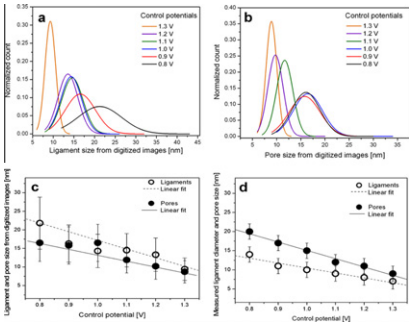

Figure 3. (a) Ligament size counts and (b) pore size counts from digitized images for the six specimens. (c) Corresponding changes in ligament and pore size vs. control potential. Ligament and pore size were taken as the peaks of each histogram. (d) Average ligament diameter and pore size as a function of the control potential. Ligament diameter and pore size were directly measured from SEM images.